Title	Design and analysis of a new multitoothed magnetless doubly salient machine
Author(s)	Lee, CHT; Chau, KT; Liu, C; Qiu, C
Citation	IEEE Transactions on Applied Superconductivity, 2014, v. 24 n. 3, article no. 5200804, p. 5200804:1-4
Issued Date	2014
URL	http://hdl.handle.net/10722/202872
Rights	IEEE Transactions on Applied Superconductivity. Copyright © IEEE.

Design and Analysis of a New Multitoothed Magnetless Doubly Salient Machine

Christopher H. T. Lee, K. T. Chau, *Fellow, IEEE*, Chunhua Liu, *Member, IEEE*, and Chun Qiu

***Abstract*—In this paper, the high temperature superconductor (HTS) winding and multitoothed structure are newly incorporated into the doubly salient (DS) and flux-switching (FS) machines, leading to create two new magnetless machines, namely the HTS-based multitoothed switched reluctance (HTS-MSR) and HTS-based multitoothed flux-switching (HTS-MFS) machines. Consequently, the design equations of the three machines, namely the MSR, HTS-MSR, and HTS-MFS, are formulated. The corresponding performances are analyzed by using the time-stepping finite element method (TS-FEM). By utilizing both torque-producing zones, the two HTS-based machines can achieve better performances than the MSR one. Moreover, the HTS-MFS can offer higher torque density than the HTS-MSR, but associated with larger torque ripple.**

***Index Terms*—Doubly salient, flux switching, high temperature superconductor, magnetless machine, multitoothed structure.**

I. Introduction

THE DEVELOPMENT of electric machines has been accelerating due to the ever increasing demand on energy efficiency and hence environmental protection. In essence, the electric machines have to offer high efficiency, high power density, high controllability, wide speed range, and maintenance-free operation [1]. To achieve these goals, the permanent-magnet (PM) machines have been actively developed. However, in recent years, the PM material cost has soared drastically while the corresponding supply is limited and fluctuating [2]. Thus, the advanced magnetless doubly salient (DS) and flux-switching (FS) machines are becoming attractive [3]. Compared with the PM machines, the magnetless DS and FS machines take the definite merit of low material cost, but suffer from relatively low torque density.

The multitoothed (multiple teeth per stator pole) switched reluctance (MSR) machine employs the flux-modulation effect to significantly improve the torque density as compared with its SR counterpart [4]. Meanwhile, the use of high-temperature superconductor (HTS) winding can readily increase the flux density and hence improve the torque density of magnetless DS and FS machines [5], [6].

The purpose of this paper is to newly incorporate the HTS winding and multitoothed structure into the DS and FS machines, hence creating two new machines: the HTS-based MSR (HTS-MSR) and HTS-based multitoothed flux-switching (HTS-MFS) machines. The design criteria and operating principles of the three magnetless machines, namely the MSR, HTS-MSR, and HTS-MFS, will be discussed. Their performances will be analyzed by using the time-stepping finite element method (TS-FEM), and then quantitatively compared.

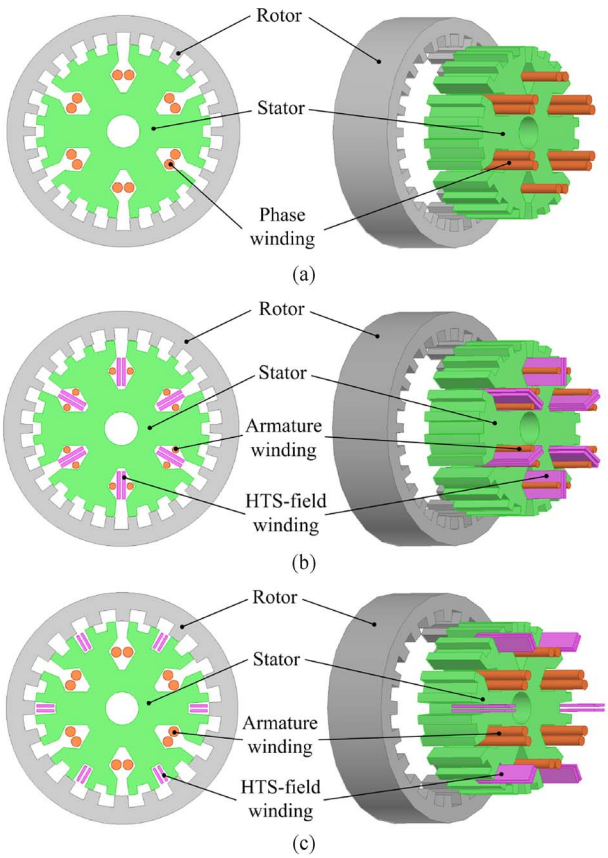

Fig. 1. Proposed machines. (a) MSR. (b) HTS-MSR. (c) HTS-MFS.

II. Machine Design

Fig. 1 shows the topologies of the three magnetless machines, namely the 24/26-pole MSR machine, the 24/26-pole HTS-MSR machine, and the 24/20-pole HTS-MFS machine. All three machines have six stator poles, each fitted with four teeth, resulting in 24 equivalent stator poles. In addition, all of them consist of the inner-stator outer-rotor topologies. The MSR machine is installed with the phase winding only, alike the conventional SR machine; meanwhile, the HTS-MSR and HTS-MFS machines adopt both armature and HTS-field windings.

Manuscript received July 13, 2013; accepted October 14, 2013. Date of publication October 21, 2013; date of current version November 8, 2013. This work was supported by the Hong Kong Research Grants Council, Hong Kong Special Administrative Region, China under (Project No. HKU 710612E).

The authors are with the Department of Electrical and Electronic Engineering, The University of Hong Kong, Pokfulam, Hong Kong (e-mail: ktchau@eee.hku.hk).

Color versions of one or more of the figures in this paper are available online at http://ieeexplore.ieee.org.

Digital Object Identifier 10.1109/TASC.2013.2286742

Since the HTS-MSR machine is derived from the MSR machine, its design equations such as the pole arrangement [4] can be extended from that of the MSR machine. Thus, the pole arrangements for both the MSR and HTS-MSR are governed by: $N_{sp} = 2mk$, $N_{se} = N_{sp}N_{st}$, $N_r = N_{se} + 2k$; where N_{sp} is the number of stator poles, N_{st} the stator teeth, N_{se} the equivalent stator poles, N_r the rotor poles, m the number of phases and k an integer. Meanwhile, the pole arrangement [6] for the proposed HTS-MFS machine can be extended from the HTS-FS machine as given by: $N_{sp} = 2mk$, $N_{se} = N_{sp}N_{st}$, $N_r = N_{se} - N_{sp} + 2k$.

In order to have a fair comparison among all three machines, the number of conduction phases and the number of multiple teeth per stator pole are kept the same. By selecting $N_{sp} = 6$, $N_{st} = 4$, $m = 3$, and $k = 1$, this ends up with $N_{se} = 24$ for all three machines. Consequently, these yield $N_r = 26$, 26 and 20 for the MSR, HTS-MSR, and HTS-MFS, respectively. Then, the machine dimensions, namely the stator diameters, rotor diameters, core lengths, pole arcs, pole heights, and yoke thicknesses, are designed in such a way that the magnetic saturation and hence the core losses can be minimized.

The key features of these three magnetless machines are summarized as follows:

- All three machines adopt the inner-stator outer-rotor structure. Hence, the inner space of the stator can be utilized to accommodate the winding.
- With the flux-modulation effect, the MSR machine can offer higher torque density than the SR counterpart. However, similar to the SR machine, the MSR still utilizes only half of its torque-producing zone, suffering from large torque ripple.
- With the use of field winding, similar to the DS and FS machines, both the HTS-MSR and HTS-MFS can utilize all the torque-producing zones, hence improving torque density and reducing torque ripple.
- To enable HTS refrigeration and isolation for the HTS-MSR and HTS-MFS, the auxiliary apparatus can readily be accommodated in the inner stator [5].
- For the HTS-MSR, both the armature and HTS-field windings are located in the same slot, thus suffering from insufficient space for winding. Meanwhile, for the HTS-MFS, these windings are located in different slots, hence easing the winding process.
- The HTS-MSR operates with a unipolar flux-linkage waveform. Meanwhile, the HTS-MFS operates with a bipolar flux-linkage waveform which results in higher torque density [3].
- According to the Meissner effect, the magnetic field in the region of HTS-field winding is virtually zero [5].

III. Operating Principle

For the MSR machine, it operates with the principle of minimum reluctance in which a unipolar rectangular current I_{MSR} is fed into the phase winding during the period of increasing self-inductance L_{MSR}. The corresponding reluctance torque T_{MSR} is always positive as shown in Fig. 2(a). However, since only half of the torque-producing zone is utilized, the torque ripple is relatively large. This reluctance torque can be expressed as [4]:

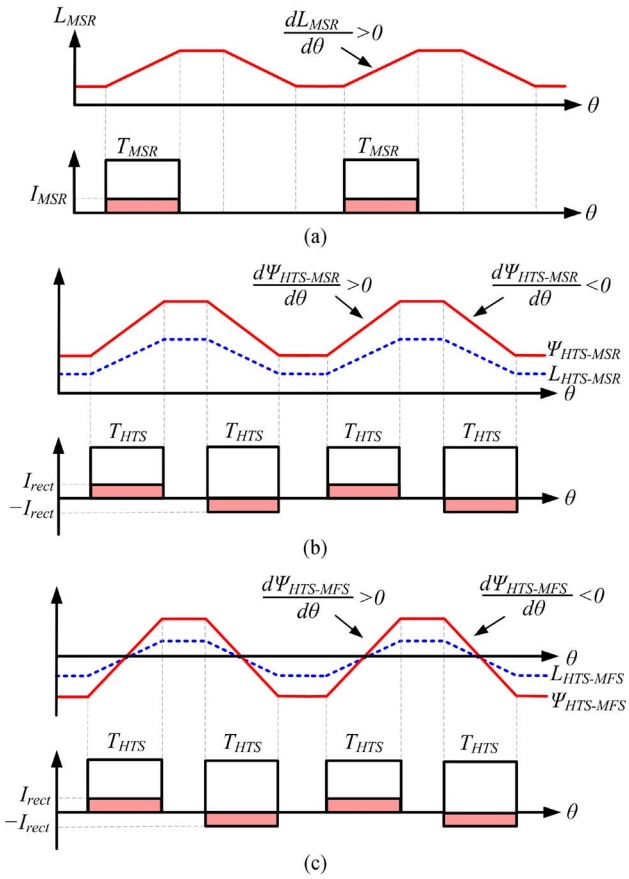

Fig. 2. Operation principles. (a) MSR. (b) HTS-MSR. (c) HTS-MFS.

$$T_{MSR} = \frac{1}{2\pi}\int_0^{2\pi}\left(\frac{1}{2}I_{MSR}^2\frac{dL_{MSR}}{d\theta}\right)d\theta. \tag{1}$$

For the HTS-MSR and HTS-MFS machines, both of them operate with a bipolar rectangular current. When the flux-linkage is increasing, a positive rectangular current I_{rect} is applied to produce a positive torque. Meanwhile, a negative rectangular current $-I_{rect}$ is applied when the flux-linkage is decreasing and the torque produced is also positive. The operating waveforms of the HTS-MSR and HTS-MFS are shown in Fig. 2(b) and (c), respectively. With this operation, two torque-producing zones are utilized and the torque ripple can be suppressed. The developed torques of these two machines are shown as:

$$T_{HTS-MSR} = \frac{1}{2\pi}\int_0^{2\pi}\left(I_{rect}\frac{d\psi_{HTS-MSR}}{d\theta} + \frac{1}{2}I_{rect}^2\frac{dL_{HTS-MSR}}{d\theta}\right)d\theta \tag{2}$$

$$T_{HTS-MFS} = \frac{1}{2\pi}\int_0^{2\pi}\left(I_{rect}\frac{d\psi_{HTS-MFS}}{d\theta} + \frac{1}{2}I_{rect}^2\frac{dL_{HTS-MFS}}{d\theta}\right)d\theta \tag{3}$$

TABLE I
MACHINE KEY DATA

	MSR	HTS-MSR	HTS-MFS
Rotor outside diameter	280.0 mm	280.0 mm	280.0 mm
Rotor inside diameter	211.2 mm	211.2 mm	211.2 mm
Stator outside diameter	210.0 mm	210.0 mm	210.0 mm
Stator inside diameter	40.0 mm	40.0 mm	40.0 mm
Airgap length	0.6 mm	0.6 mm	0.6 mm
Stack length	80.0 mm	80.0 mm	80.0 mm
No. of phases	3	3	3
No. of armature turns	80	50	80
HTS-field material	N/A	BSCCO-2223	BSCCO-2223

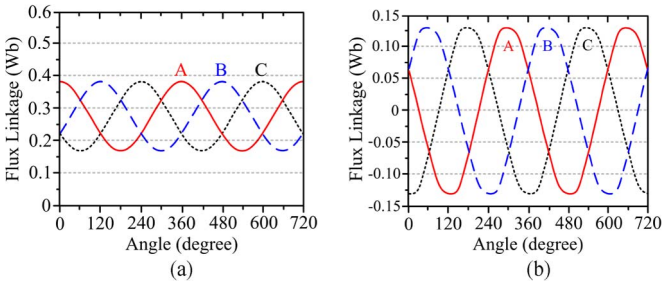

Fig. 3. Flux linkages. (a) HTS-MSR. (b) HTS-MFS.

where $\Psi_{HTS-MSR}$ and $\Psi_{HTS-MFS}$ are the flux-linkages of the HTS-MSR and HTS-MFS, respectively, and $L_{HTS-MSR}$ and $L_{HTS-MFS}$ are their self-inductances. It should be noted that the developed torque is mainly contributed by HTS-field torque component, whereas the reluctance torque component has an averaged zero value.

IV. PERFORMANCE ANALYSIS

All the three magnetless machines are analyzed under the same stator diameters, rotor diameters, stack lengths, and airgap lengths. Meanwhile, due to insufficient space to accommodate two types of windings per slot, the number of armature coils for the HTS-MSR is less than its counterparts. The key design data of these machines are listed in Table I. By using the TS-FEM, all machine performances can be simulated and then quantitatively compared.

First of all, the flux-linkages of HTS-MSR and HTS-MFS are shown in Fig. 3. It can be seen that both flux-linkages are well balanced among three phases without noticeable distortion. These confirm that the design data of these two machines are correct. In addition, the results confirm that the HTS-MSR exhibits the unipolar flux-linkage waveform while the HTS-MFS has the bipolar flux-linkage waveform.

Secondly, the peak values of the no-load electromotive force (EMF) of the HTS-MSR and HTS-MFS at the rated speed versus the HTS-field excitation are plotted in Fig. 4. It can be observed both machines perform similarly with their no-load EMFs increasing with the HTS-field excitation; however, the HTS-MSR saturates faster than the HTS-MFS counterpart. This is due to the fact the HTS-MFS allows for bipolar flux-linkage which can significantly enlarge the range of flux variation for the same saturation level of iron core.

In the third place, the no-load EMFs of the HTS-MSR and HTS-MFS under the HTS-field excitation of 500 A-turn are

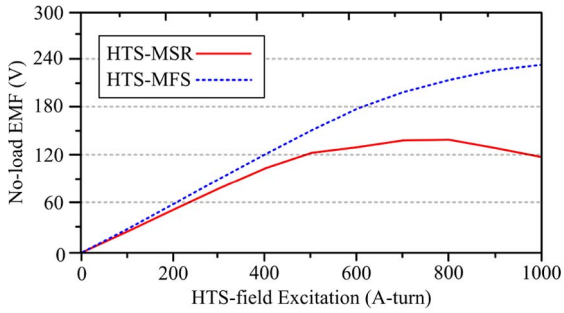

Fig. 4. Peak values of no-load EMF versus HTS-field excitation.

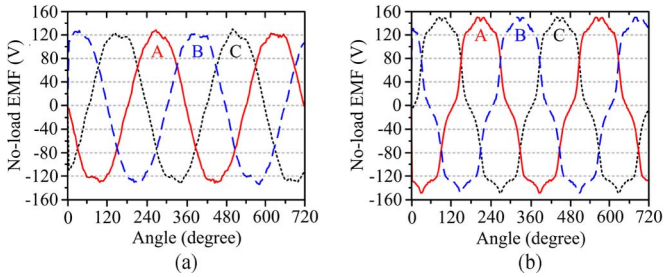

Fig. 5. No-load EMFs at HTS-field 500 A-turn. (a) HTS-MSR. (b) HTS-MFS.

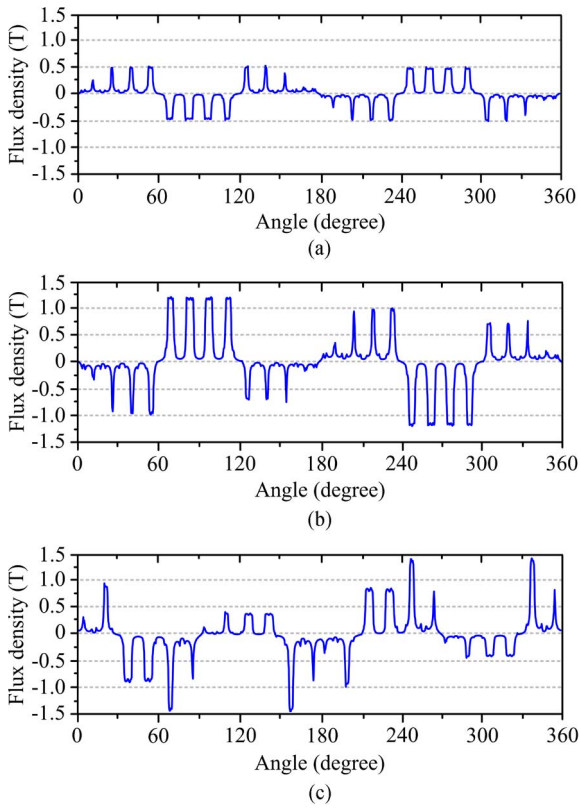

Fig. 6. Airgap flux densities. (a) MSR. (b) HTS-MSR. (c) HTS-MFS.

shown in Fig. 5. The results show that the HTS-MSR exhibits more sinusoidal and symmetrical waveforms than the HTS-MFS. Hence, the HTS-MSR can offer lower torque ripple than the HTS-MFS.

In the fourth place, the airgap flux density distributions of three machines at full load are calculated as shown in Fig. 6. It shows that the original flux of each stator pole of all machines is

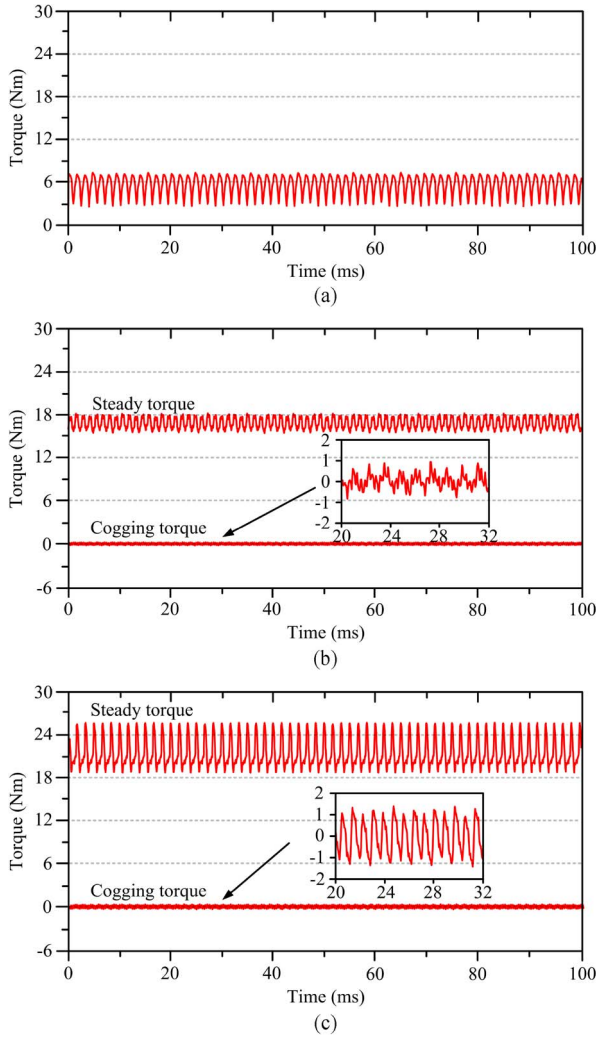

Fig. 7. Torque performances. (a) MSR. (b) HTS-MSR. (c) HTS-MFS.

modulated into four portions in accordance with the number of teeth per stator pole. These verify that the proposed machines can offer the flux-modulation effect, hence boosting up the torque density accordingly.

Fifthly, the output torque waveforms of the machines are simulated as shown in Fig. 7. It can be observed that the average torques of the MSR, HTS-MSR and HTS-MFS machines are 5.64 Nm, 15.7 Nm and 22.1 Nm, respectively. Compared with the MSR machine, the torque enhancement of the HTS-MSR and HTS-MFS machines are 178.4% and 291.8%, respectively. Meanwhile, the peak amplitude of the cogging torque of the HTS-MSR and HTS-MFS are 1.6 Nm and 2.6 Nm, respectively. These values are very acceptable, which are only 10.2% and 11.8% of their rated torques. It can also be observed that the torque ripples of the MSR, HTS-MSR and HTS-MFS machines are 64.3%, 19.6% and 31.6%, respectively, which are comparable with the SR, DS and FS machines, respectively [1].

It should be noted that the cogging torque is the detent torque due to the interaction between the rotor and the stator teeth in the presence of HTS-field excitation. So, it can be considered as the torque at no-load condition. Meanwhile, the torque ripple is a measure of torque fluctuation which is defined as the ratio of the peak-to-peak torque difference to the average torque.

TABLE II
MACHINE PERFORMANCE COMPARISON

	MSR	HTS-MSR	HTS-MFS
Power	300 W	830 W	1160 W
Rated speed	500 rpm	500 rpm	500 rpm
Field excitation	N/A	500 A-turn	500 A-turn
No-load EMF	N/A	122 V	148 V
Airgap flux density	0.48 T	1.23 T	1.38 T
Rated torque	5.64 Nm	15.7 Nm	22.1 Nm
Torque enhancement	N/A	178.4 %	291.8 %
Cogging torque	N/A	1.6 Nm	2.6 Nm
Torque ripple	64.3 %	19.6 %	31.6 %
Core loss	10.1 W	20.4 W	24.6 W

V. CONCLUSION

In this paper, three advanced magnetless DS machines, namely the MSR, HTS-MSR, and HTS-MFS have been analyzed and quantitatively compared. With the flux-modulation effect, all three multitoothed machines can boost up their torque levels. The comparison is summarized in Table II which concludes that the HTS-based machines have higher torque densities than the MSR counterpart. Nevertheless, they suffer from higher core losses than the MSR one. The HTS-MFS exhibits the best performances in terms of the power density, torque density, but suffers from larger cogging torque and torque ripple than the HTS-MSR one. Particularly, both HTS-based machines, especially the HTS-MFS, can offer the torque density comparable with the PM machines. Because of the ever increasing cost and limited supply of the PM material, the magnetless HTS-based machines are becoming more and more promising. The three machines are under prototyping and the experimental data will be the substance of our future papers. Finally, the HTS-based machines should be designed at the megawatt range so as to justify the additional HTS apparatus. Also, they will become more economical than the PM machines [2] at this power range.

REFERENCES

[1] K. T. Chau, W. Li, and C. H. T. Lee, "Challenges and opportunities of electric machines for renewable energy," *Progr. Electromagn. Res. B*, vol. 42, pp. 45–74, 2012.
[2] J. Li and K. T. Chau, "Performance and cost comparison of permanent-magnet vernier machines," *IEEE Trans. Appl. Supercond.*, vol. 22, no. 3, p. 5202304, Jun. 2012.
[3] Z. Q. Zhu, "Switched flux permanent magnet machines—Innovation continues," in *Int. Conf. Elect. Mach. Syst.*, 2011, pp. 1–10.
[4] C. H. T. Lee, K. T. Chau, C. Liu, D. Wu, and S. Gao, "Quantitative comparison and analysis of magnetless machines with reluctance topologies," *IEEE Trans. Magn.*, vol. 49, no. 7, pp. 3969–3972, Jul. 2013.
[5] C. Liu, K. T. Chau, J. Zhong, and J. Li, "Design and analysis of a HTS brushless doubly-fed doubly-salient machine," *IEEE Trans. Appl. Supercond.*, vol. 21, no. 3, pp. 1119–1122, Jun. 2011.
[6] Y. Wang, J. Sun, Z. Zou, Z. Wang, and K. T. Chau, "Design and analysis of a HTS flux-switching machine for wind energy conversion," *IEEE Trans. Appl. Supercond.*, vol. 23, no. 3, p. 5000904, Jun. 2013.